Band-gap evolution, hybridization, and thermal stability of $In_xGa_{1-x}N$ alloys measured by soft X-ray emission and absorption

Philip Ryan,* Cormac McGuinness, James E. Downes, and Kevin E. Smith†
Department of Physics, Boston University, Boston, Massachusetts 02215

Dharanipal Doppalapudi and Theodore D. Moustakas
Electrical and Computer Engineering Department, Boston University, Boston, Massachusetts 02215
(Received 15 November 2001; published 24 April 2002)

The electronic structure of $In_xGa_{1-x}N$ alloys with ($0 \leqslant x \leqslant 0.3$) has been studied using synchrotron radiation excited soft x-ray emission and absorption spectroscopies. These spectroscopies allow the elementally resolved partial density of states of the valence and conduction bands to be measured. The x-ray absorption spectra indicate that the conduction band broadens considerably with increasing indium incorporation. The evolution of the band gap as a function of indium content derives primarily from this broadening of the conduction-band states. The emission spectra indicate that motion of the valence band makes a smaller contribution to the evolution of the band gap. This gap evolution differs from previous studies on the $Al_xGa_{1-x}N$ alloy system, which observed a linear valence-band shift through the series ($0 \leqslant x \leqslant 1$). For $In_xGa_{1-x}N$ the valence band exhibits a large shift between $x=0$ and $x=0.1$ with minimal movement thereafter. We also report evidence of In $4d-N\ 2p$ and Ga $3d-N\ 2p$ hybridization. Finally, the thermal stability of an $In_{0.11}Ga_{0.89}N$ film was investigated. Both emission and absorption spectra were found to have a temperature-dependent shift in energy, but the overall definition of the spectra was unaltered even at annealing temperatures well beyond the growth temperature of the film.

DOI: 10.1103/PhysRevB.65.205201 PACS number(s): 78.70.En, 78.70.Dm, 71.20.Nr, 71.55.Eq

I. INTRODUCTION

Nitride based wide band-gap semiconductors have great technological potential due to their application in light-emitting devices coupled with their extreme hardness and the ability to sustain high temperatures.[1–5] The band-gap energies of InN, GaN, and AlN, are 1.9, 3.4, and 6.2 eV, respectively, and optoelectronic devices made from alloys of these nitrides cover the visible to ultraviolet range of the electromagnetic spectrum.[6] $In_xGa_{1-x}N$ and $Al_xGa_{1-x}N$ alloys have successfully been grown and their band-gap energies found to vary with In or Al concentration. However, experimental data on the detailed electronic structure of these alloys is scarce, particularly in the case of $In_xGa_{1-x}N$. While photoemission spectroscopy is a standard probe of electronic structure in solids, it is difficult to apply to $In_xGa_{1-x}N$ since it requires that atomically clean surfaces be prepared before bulk properties can be measured.[7–9] Successful methods exists for cleaning surfaces of thin film GaN, but obtaining clean surfaces of $In_xGa_{1-x}N$ alloys suitable for photoemission studies is very difficult.[10] However, soft x-ray emission (SXE) and soft x-ray absorption (SXA) spectroscopies are ideal probes of the valence- and conduction-band density of states since these spectroscopies have a sampling depth of $\approx$1000 Å, and are thus insensitive to atomic contamination or disorder of sample surfaces.[11] We previously have used SXE and SXA to study the electronic structure of GaN and $Al_xGa_{1-x}N$ alloys, and were able to measure the elementally resolved partial density of states (PDOS), the band-gap evolution as a function of $Al_xGa_{1-x}N$ composition, and shallow core-level hybridization.[12–14]

We present here an SXE and SXA study of electronic structure in $In_xGa_{1-x}N$, and report the first full measurement of the elementally resolved valence- and conduction-band PDOS in this alloy system. SXA indicates that the conduction band broadens considerably with increasing In content. We find that the band-gap evolution as a function of indium content derives primarily from this broadening of the conduction-band states for $x>0.1$. The SXE spectra indicate that motion of the valence band makes a smaller contribution to the evolution of the band gap for $x>0.1$. The change in the band gap between $x=0$ and $x=0.1$ appears to be dominated by the motion of the valence band. This gap evolution differs from that in $Al_xGa_{1-x}N$, where a linear valence-band shift through the series ($0 \leqslant x \leqslant 1$) was observed.[14] We also measured In $4d-N\ 2p$ and Ga $3d-N\ 2p$ shallow core-level hybridization throughout the alloy series, and measured the thermal stability of an $In_{0.11}Ga_{0.89}N$ film. Both SXE and SXA spectra shifted in energy with temperature, but the overall definition of the spectra was unaltered even at annealing temperatures well beyond the growth temperature of the film.

II. EXPERIMENTAL DETAILS

The samples of $In_xGa_{1-x}N$ ($0 \leqslant x \leqslant 0.29$) investigated were wurtzite thin films of thickness 1.2, 1.1, 0.5, and 0.25 μm for $x=0$, 0.1, 0.2, and 0.29, respectively. Samples were grown by electron cyclotron resonance excited molecular-beam epitaxy on *A*-plane $(1\bar{1}20)$ sapphire in a three-step process. First the sapphire surface was converted from aluminum oxide to AlN by exposing it to a microwave nitrogen plasma for $\approx$20 min. Next, a GaN buffer layer of about 300 Å was grown at 550 °C. Finally the $In_xGa_{1-x}N$ alloy layer is grown at 650–675 °C. The $In_xGa_{1-x}N$ films are autodoped *n*

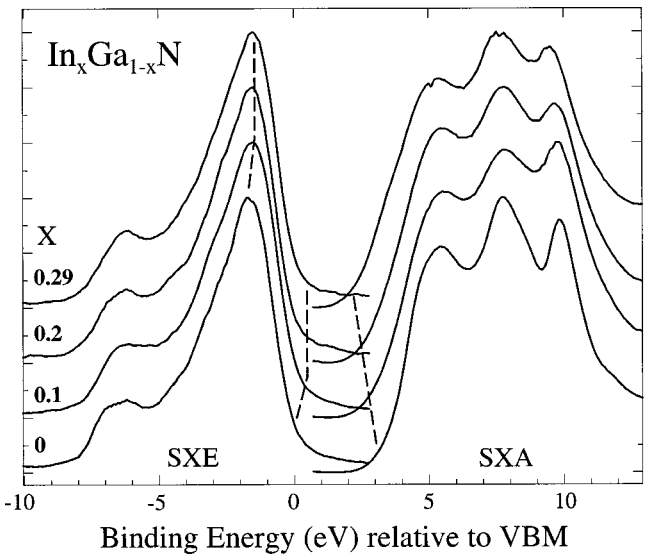

FIG. 1. N $2p$ SXE and SXA spectra from a series of $In_xGa_{1-x}N$ alloys. The energy axis is set with respect to the valence-band maximum (VBM) of GaN ($x=0$). The absorption spectra shown here were taken at grazing incidence. $h\nu_{exc}=408$ eV for the SXE spectra.

type. All the films were grown with c axis [0001] perpendicular to substrate surface, based on x-ray diffraction (XRD) and electron microscopy studies. Further details of the growth conditions and the structure of the films have been reported elsewhere.[15,16] The films were characterized by XRD and photoluminescence; XRD was also used to obtain the In and Ga ratios and to ascertain whether any phase separation is present.[15]

The SXE and SXA experiments were performed on the undulator beam line X1B at the National Synchrotron Light Source, Brookhaven National Laboratory. Absorption spectra were recorded either in the total electron yield mode by measuring the sample drain current or by the total fluorescent yield mode, and were taken with energy resolutions of ≈0.2 at 400 eV (in the vicinity of the N $1s$ edge) and of 0.8 eV at 1116 eV (in the vicinity of the Ga $2p$ edge). Emission spectra were recorded using a Nordgren-type grazing-incidence grating spectrometer using a 5-m 1200-lines/mm grating in first order of diffraction at a resolution of ≈0.31 eV at the N $1s$ edge.[11,17–19] To detect Ga $2p$ emission (~1000 eV) the spectrometer used second-order diffraction with a resolution of ~0.9 eV. The acquisition time for individual SXE spectra was ≈90 min. The base pressure in the experimental system was better than 1.0×10^{-9} Torr. Sample surfaces were not processed or cleaned in the vacuum chamber. Details of the energy calibration for the SXE and SXA spectra can be found elsewhere.[12,14]

III. RESULTS AND DISCUSSION

A. Valence- and conduction-band PDOS and band-gap evolution

Figure 1 presents the SXE and SXA spectra for the N $2p$ occupied and unoccupied states, respectively, for a series of

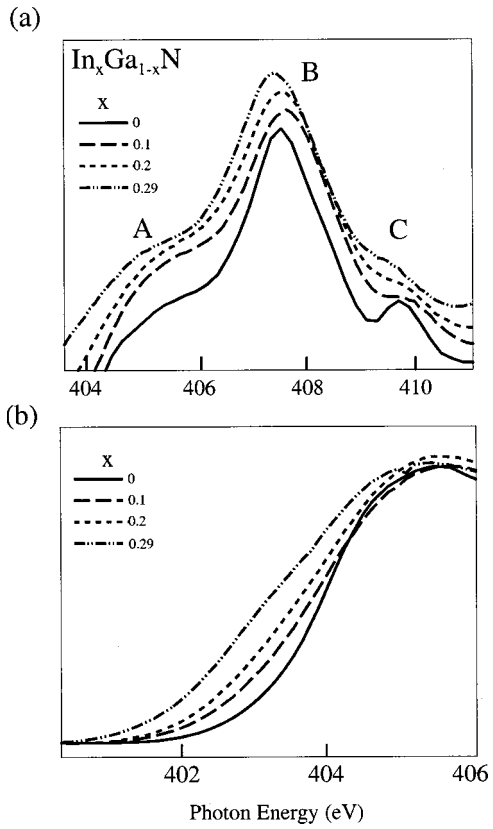

FIG. 2. Normal-incidence SXA spectra for $In_xGa_{1-x}N$ as a function of In content. Panel (a) shows the shift in the main spectral features, panel (b) shows the motion of the conduction-band minimum.

$In_xGa_{1-x}N$ alloys. The dashed lines indicate movements of the band edges as a function of indium content. The energy axis is referenced to the valence-band maximum (VBM) of GaN, which is estimated by linearly extrapolating the leading edges of the absorption and emission spectra and the band gap is set to the bulk value of 3.4 eV. (A similar linear extrapolation was successfully used in our earlier study of $Al_xGa_{1-x}N$ alloys.[14]) The sample series is limited due to the difficulty in growing high-quality $In_xGa_{1-x}N$ with an indium content beyond $x=0.35$, as the sample begins to phase separate into both InN and GaN.[15] (Note that the SXE and SXA spectra of the binary nitride compounds have been reported previously.[12,14,20]) The evolution of the elementally resolved band gap in the $In_xGa_{1-x}N$ alloy system is clearly visible in Fig. 1. Unlike the behavior of $Al_xGa_{1-x}N$ alloys,[14] the shift in the top of the N $2p$ valence band in $In_xGa_{1-x}N$ is not linear with x. Figure 1 reveals a shift of the top of the N $2p$ valence-band emission of 0.15 eV between the GaN ($x=0$) and $In_{0.1x}Ga_{0.9}N$, but no further shift in the band edge as the In content is increased. This is consistent with the results of large supercell empirical pseudopotential calculations, which predict a large shift of the VBM between $x=0$ and $x=0.1$, with a much smaller shift thereafter.[21] In contrast to the measured behavior of the VBM, the N $2p$ conduction-band edge shown in the SXA spectra of Fig. 1 shifts continuously with In content. This is highlighted in Fig. 2, where the SXA spectra were recorded at normal incidence. Three broad fea-

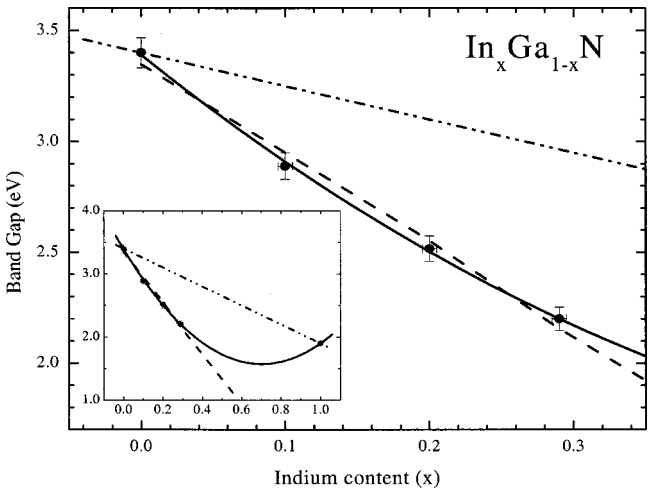

FIG. 3. Evolution of the band gap for the N $2p$ PDOS in $In_xGa_{1-x}N$ as a function of In content, as measured from the SXE and SXA spectra in Fig. 1. Data points indicate the position of the experimentally determined gap, the solid line is the fit using Vegard's law with a constant bowing parameter of $b=3.68$ eV, the dashed line is a straight-line fit to the data points for $0\leqslant x\leqslant 0.29$, the dash-dot line is the predicted position if the bowing parameter b is zero. See text for details.

tures (labeled *A*, *B*, and *C*) can be identified, and the motion of the conduction-band edge with increasing In content is clearly visible. This is also consistent with the supercell calculations.[21] Figure 2(b) reveals that the motion of the edge derives mostly from the broadening of spectral feature *A*. (This broadening of the SXA edge has also been noted in a N *K* NEXAFS measurement from an $In_{0.16}Ga_{0.84}N$ alloy.[22]) The observed behavior of the experimentally measured N $2p$ band gap derived from the SXE and SXA spectra of Fig. 1 is plotted in Fig. 3. The solid line is a least-squares quadratic fit through the data points, the dashed line is a linear fit through the $In_xGa_{1-x}N$ ($0\leqslant x\leqslant 0.3$) data points, and the dash-dot line is a straight extrapolation from the GaN to InN bulk band-gap values. A significant deviation from linear gap evolution is evident. Theoretically, the behavior of the energy gap in such an alloy system may be described by Vegard's law,[23]

$$E_g(x)=\overline{E}_g+\Delta E_g(x-\tfrac{1}{2})-bx(1-x).$$

Here, $\overline{E}_g$ is the average gap, ΔE_g is the difference between the gaps of the pure end members of the alloy system, and b is the bowing parameter. The bowing parameter allows for deviation from the linear behavior of the band gap, and from the fit to the data presented here, a value for $b=3.68$ eV is obtained. However although Vegard's law can be fitted satisfactorily to the range of data presented here, the large bowing parameter obtained would result in the value of the InN gap being reached at $x=0.41$, where b is held constant. As can be seen in Fig. 3, the measured band gap for the $In_xGa_{1-x}N$ alloys ($x\leqslant 0.3$) exhibits a pseudolinear dependence on the In fraction, x. A linear least-squares fit to the band-gap data for $x\leqslant 0.3$ gives

$$E_g=3.35-4.04x.$$

This figure is comparable to a number of recent studies of $In_xGa_{1-x}N$ epilayers, which obtained slopes with values of -3.57, -3.86, and -3.93.[24–27] As will be discussed below, the linear fit to the data does not appear to be as satisfactory as the quadratic fit using the Vegard's law expression.

A review of the band parameters for III-V compound semiconductors and their alloys gives an overview of the theoretical and experimental results obtained for the bowing parameter and provisionally suggests a bowing coefficient of 3.0 eV.[28] First-principle calculations of the bowing parameter in $In_xGa_{1-x}N$ have varied from $b=1.02$,[29] $b=1.16$,[30] $b=2.6$ eV,[31] to $b=3.5$ eV.[26,27] Many of these calculations have been performed for the zinc-blende phase, but band-gap bowing in the wurtzite phase has been expected to be very similar.[29] Likewise, experimental results have varied with band-gap bowing values ranging initially from $b=1$ eV,[32] to $b=2.6$–4.11 eV.[26,30,33,34] Some studies of low In content $In_xGa_{1-x}N$ alloys ($x<0.1$) have indicated large bowing parameters and composition-dependent band-gap bowing coefficients.[26,33] The supercell empirical pseudopotential calculations of Bellaiche *et al.* produce a bowing parameter that has a strong composition dependence, with $b>5$ eV for small ($x<0.1$) compositions.[21] The calculations also predict strong shifts in the VBM, particularly at small x, and much smaller shifts in the conduction-band minimum. We measure a behavior similar to these predictions, but interpolating the results of the calculation to obtain the bowing parameters for the In fractions of the alloys studied here gives band gaps that are smaller than we measure at $x=0.1$, and larger than we measure at $x=0.29$.

The discrepancy between earlier experimental results, which indicated small bowing parameters, and more recent studies that indicate large bowing parameters, has been partly ascribed to erroneous estimates of the alloy composition favoring the large bowing factors, or conversely that the more recent photoluminescence emission may have resulted from local fluctuations in the In fraction, which could lead to overestimates of the bowing parameter.[28] However, a study of $In_xGa_{1-x}N$ alloys using a wide range of experimental techniques resulted in a large spread of gap values for samples with $x<0.4$.[35] The bowing coefficient for the band gap obtained from this data set was $b=2.5$ eV. A linear fit to the same data set gives a slope of -3.2 eV for the variation of the calculated band gap with In content. As noted above, however, our results give a bowing coefficient of $b=3.68$ eV and a slope of -4.04 eV.

It has been suggested that the bowing term $x(1-x)$ is reasonable only when based on the assumption that the mixed crystal is an ideal solution and the crystal lattice changes gradually through the ternary alloy system.[36] While phase separation is well documented in $In_xGa_{1-x}N$ alloys with high indium content,[15,37,38] a valence force-field calculation of a relatively low indium content ($In_{0.2}Ga_{0.8}N$) model alloy revealed random alloying or ''alloy disorder'' as opposed to complete phase separation.[39] Due to the In-N and Ga-N bond-length difference ($\sim$10.8%), the atomic positions are considered to fluctuate from the ideal lattice sites, leaving

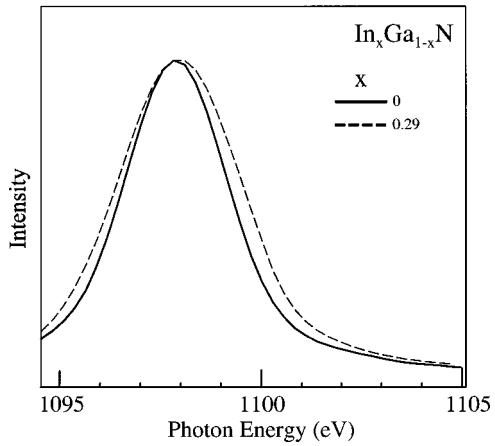

FIG. 4. Ga L_α SXE spectra for GaN and $In_{0.29}Ga_{0.71}N$. The peak is due to transitions from the Ga $3d$ core level (19 eV below the VBM) to the Ga $2p_{3/2}$ core level. See text.

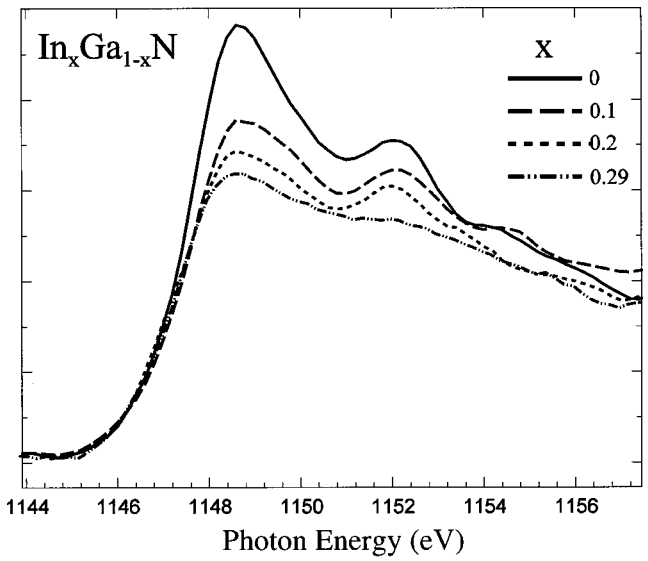

FIG. 5. Total electron yield Ga L SXA spectra of the $In_xGa_{1-x}N$ series, revealing the Ga-derived conduction-band PDOS.

both bond-length and bond-angle distortions in the alloy. Others have suggested that the large, composition-dependent band-gap bowing coefficient along with other optical anomalies in $In_xGa_{1-x}N$ alloys are due to the localization of hole states in the upper valence band.[21] Bellaiche *et al.* point out that, in contrast to conventional alloys, no chemical clustering of In atoms is needed to induce this localization. Thus the results presented here can reasonably be interpreted as obtained from random alloys rather than from the existence of phase-separated InN.

While N $2p$ states dominate the top of the valence band, the bottom of the conduction band is a mixture of Ga $4s$, Ga $4p$, and N $2p$ states. Furthermore, there are occupied Ga $3d$ and N $2s$ states just below the valence band, and Ga $4s$ and $4p$ states mixed into the valence band itself. Figure 4 shows the SXE spectra resulting from transitions from the Ga $3d$ states to the Ga $2p_{3/2}$ state for some of the series of $In_xGa_{1-x}N$ alloys studied ($h\nu_{exec}=1150$ eV). The full width at half maximum (FWHM) of the Ga $3d$ emission from pure GaN was 3.13 eV, and did not change for the 10% In alloy. However, the Ga $3d$ FWHM increased to 3.59 eV for $In_{0.2}Ga_{0.8}N$ and 3.71 eV for $In_{0.29}Ga_{0.71}N$. This is clearly visible in Fig. 4, which shows the spectra for GaN and $In_{0.29}Ga_{0.71}N$. Figure 5 presents the SXA spectra for absorption from the Ga $2p_{3/2}$ level into the conduction band. The absorption data show a clear loss of spectral feature definition as the In content increases. These changes, and the increase in FWHM of the Ga $3d$ emission, are consistent with the speculated alloy disordering.[39]

B. Hybridization of N $2p$ states with Ga $3d$ and In $4d$ states in $In_xGa_{1-x}N$

SXE has been shown to be highly sensitive to hybrid states.[12,14] This is a consequence of the strong dipole selection rules that govern the transitions, and the dominance of intra-atomic transitions over interatomic transitions. In particular, it was found that SXE was able to measure the hybridization of N $2p$ states with Ga $3d$ states in $Al_xGa_{1-x}N$ alloys, and follow the changes in the strength of hybridization as a function of Ga content in the alloys.[14] The Ga $3d$ state lies $\approx$19 eV below the valence-band maximum. When N $2p$-$1s$ SXE spectra were recorded from GaN or $Al_xGa_{1-x}N$, a weak emission feature was observed at this energy, which could be conclusively identified as emission from N $2p$ states hybridized with the Ga $3d$ shallow core level.[14] Figure 6 shows a series of N $2p$-$1s$ SXE spectra from $In_xGa_{1-x}N$. These are the same spectra as presented in Fig. 1, but the energy scale is expanded to show emission up to 30 eV below the VBM. As can be seen in the spectrum for pure GaN ($x=0$) in Fig. 6, there is a clear emission feature at $\approx$19 eV due to the N $2p-$Ga $3d$ hybridization. As the In content increases, the emission feature at 19 eV decreases, due to the reduction in relative Ga content. This is identical to the behavior seen in $Al_xGa_{1-x}N$.[14] However, in $In_xGa_{1-x}N$ the Ga atoms are being substituted by an element that has shallow d states of its own, which is not the case for $Al_xGa_{1-x}N$. Thus while we anticipate a reduction in N $2p$ hybridization to Ga $3d$ states as the Ga content decreases, we also anticipate an increase in hybridization of N $2p$ states to In $4d$ states as the In content increases. Such a behavior is evident in Fig. 6, where it is clear that as the emission feature at $\approx$19 eV decreases with In content, a feature at approximately 17 eV increases. The resolution used and the weak nature of the signal lead to the apparent overlap of these two emission features, and preclude any meaningful fitting of the hybrid features for the high In content alloys. As in the case of $Al_xGa_{1-x}N$, this hybridization of the shallow core levels is important, since it must be taken into account when band-structure calculations are performed.

C. Angle-dependent SXA spectra

X-ray absorption spectra can display strong intensity variations as a function of the angle of incidence of the radiation. This is a consequence of the linearly polarized nature of the synchrotron radiation used in the experiment. The

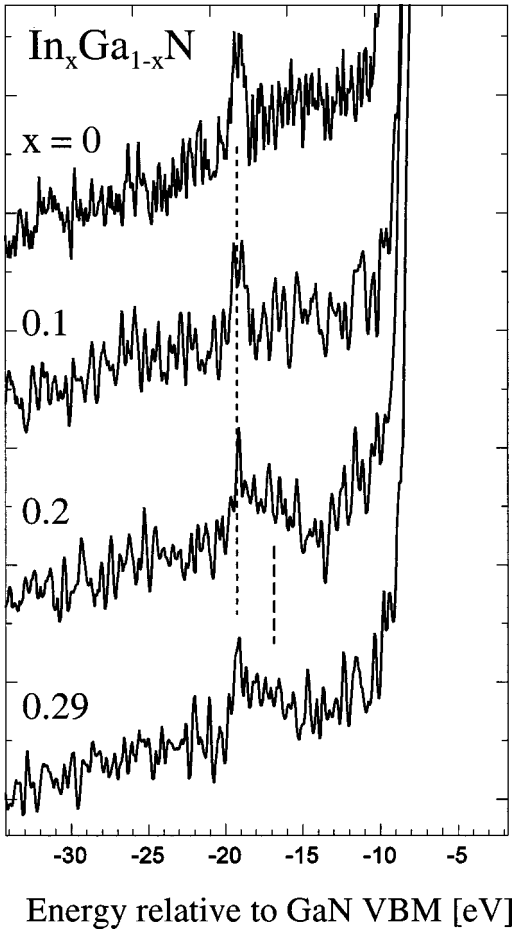

FIG. 6. N *K* emission spectra from $In_xGa_{1-x}N$ ($0 \leqslant x \leqslant 0.29$). This is the same SXE data as in Fig. 1, but the emission below the main valence band is shown. The emission at 19 eV below the GaN VBM originates from N $2p$ states hybridized with Ga $3d$ states. This feature weakens as the relative Ga content is reduced. A second very weak feature at 17 eV develops as the In content increases. This feature is due to N $2p$ states hybridized with In $4d$ states

transition matrix element **M** in the x-ray absorption process contains the scalar product of the polarization vector of the incoming photon **e** and the position vector of the electron **r**

$$\mathbf{M} = \langle \phi_{1s} | \mathbf{e} \cdot \mathbf{r} | \phi_f \rangle,$$

where here we use φ_{1s} for the wave function of a N $1s$ electron and φ_f is the wave function of the final state into which the $1s$ electron is excited.[40] The dipole transition operator $\mathbf{e} \cdot \mathbf{r}$ projects out the orbitals along the direction of the polarization vector. Thus SXA spectral intensities reflect orbital symmetries. For the wurtzite films studied here, the c axis coincides with the film normal. Consequently, the p_z (out-of-plane) orbitals are excited at *K* edges (absorption from $1s$ states) when $\mathbf{e} \perp c$. Similarly, the $p_{x,y}$ (in-plane) orbitals are preferentially excited when $\mathbf{e} \| c$. Such effects have been reported earlier by Lawniczak-Jablonska *et al.* for N *K* absorption in the binary III nitrides AlN, GaN, and InN.[41] They have also been reported for the $Al_xGa_{1-x}N$ alloys.[14]

Figure 7 shows the angular dependence of the N $1s$-$2p$ SXA spectra for GaN ($x=0$) and $In_{0.29}Ga_{0.71}N$. Each of the

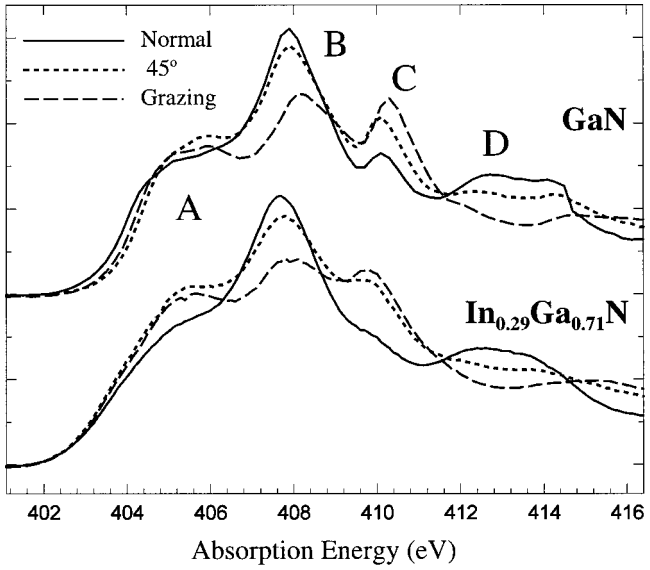

FIG. 7. Polarization effects on SXA spectra in $In_xGa_{1-x}N$. Spectra are shown for $x=0$ and $x=0.29$. The origin of the labeled features is discussed in the text.

four labeled absorption features shows changes in intensity and energy as the angle of incidence of the synchrotron radiation is varied. The normal-incidence spectrum represents the situation of $\mathbf{e} \perp c$, while the grazing-incidence spectrum approximately represents $\mathbf{e} \| c$. Just as was found for $Al_xGa_{1-x}N$,[14] the orientation dependence in N $1s$-$2p$ SXA for the $In_xGa_{1-x}N$ alloys reveals that the grazing-incidence geometry spectra generally have less pronounced and weaker features than those for normal incidence. This is consistent with the stronger in-plane and weaker out-of-plane bonding expected by the crystal structure. The spectra were normalized to have equal intensity before the edge and far above the conduction band. The polarization dependence of SXA spectra for cubic and hexagonal InN, AlN and GaN has been investigated earlier.[41] While the cubic structures indicated little polarization dependence, the hexagonal structures showed a cation dependent angular distribution.[41] Figure 7 shows angular changes for GaN and $In_{0.29}Ga_{0.71}N$ that are much weaker than reported for pure InN.[41] The behavior of the anisotropy is very similar for all In concentrations. The main part of the conduction band is about (12–14) eV wide and we identify four pronounced features (denoted A–D). The N *K*-absorption spectra for GaN and $In_{0.29}Ga_{0.71}N$ are similar, with the in-plane character strongest at energies around 5 eV (feature *B*). The influence of Al in $Al_xGa_{1-x}N$ can be contrasted with that of In in $In_xGa_{1-x}N$. For $Al_{0.5}Ga_{0.5}N$, there a shift to higher energies of the out-of-plane component of feature *B*, while for $In_{0.29}Ga_{0.71}N$ the feature moves to lower energy.[14]

D. Thermal effects

As noted earlier, $In_xGa_{1-x}N$ alloys have a propensity to phase separate, particularly at high indium content.[15,37,38] A growth phase diagram formulated by Ho and Stringfellow illustrates the growth stability of the InN-GaN quasibinary

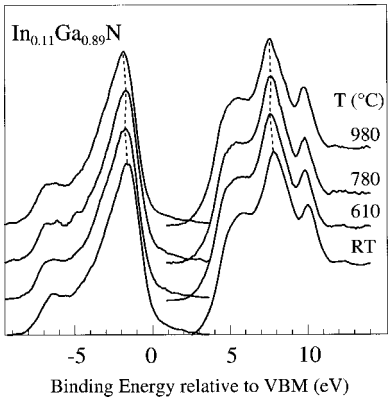

FIG. 8. SXE and SXA spectra showing the N $2p$ PDOS of both the valence and conduction bands of an $In_{0.111}Ga_{0.89}N$ sample as a function of annealing temperature. RT indicates room temperature. See text.

system with respect to indium content and growth temperatures.[42,43] From this formulation the stability of the grown crystal may be predicted. Doppalapudi *et al.* grew samples both in the stable and unstable regions of the phase diagram and verified the predictions using x-ray diffraction measurements.[15] We used SXE and SXA to study thermal effects on the band structure of a film grown in the stable region of the phase diagram. A sample of $In_{0.11}Ga_{0.89}N$ was heated to three temperatures: 610, 780, and 980 °C. The sample growth temperature was $\approx$650–675 °C, thus these sample temperatures were, respectively, below, near, and well above the growth temperature. In each case the sample was heated for an hour at each temperature and then cooled to room temperature and the SXE and SXA spectra were recorded. The annealing procedure was performed in vacuum at $\sim 1\times10^{-8}$ Torr.

Figure 8 shows the emission and absorption spectra of the N $2p$ valence- and conduction-band density of states through the annealing series. The qualitative features of the spectra are unaffected, with almost no broadening effects, but upon close inspection, a slight shift in both the valence-band and conduction-band edges is evident. This shift of the spectra is indicated by the dashed lines in Fig. 8. After annealing to 610 °C both the spectra exhibit a decrease in energy. Annealing to 780 °C resulted in no further spectral shift. But another energy shift (to a lesser extent in the absorption spectra) is evident after annealing to 980 °C. The stability of the bands at high temperatures is evident from the constant spectral shape. The band shifting sequence or origin is not understood at present.

IV. CONCLUSIONS

We have studied the electronic structure of $In_xGa_{1-x}N$ alloys using soft x-ray absorption and emission spectroscopies x between 0 and 0.3. The N $2p$ valence band shows very little change with increasing indium content. The elementally resolved N $2p$ band-gap evolution as a function of In content was measured, and found to differ significantly from that observed for $Al_xGa_{1-x}N$. A 0.15-eV shift of the VBM in the N $2p$ SXE between $x=0$ and $x=0.1$ is observed, but no significant movement thereafter. This is in good agreement with calculations that attribute this behavior and the anomalous compositional-dependent band-gap bowing to In-localized hole states in the upper valence band.[21] The SXA spectral features broaden with increasing In content, indicating a decrease in the atomic nitrogen localization, primarily caused by the random alloying in the crystal.[14] Finally, the thermal stability of an $In_{0.11}Ga_{0.89}N$ sample was investigated and indicated stability at elevated temperatures beyond the growth temperature of the crystal.[42,43]

ACKNOWLEDGMENTS

This work was supported in part by the National Science Foundation under Grant No. DMR-99-86099 and the U.S. Army Research Office under Grant No. 40126-PH. Our x-ray emission spectrometer is funded by the U.S. Army Research Office under Grant No. DAAH04-95-0014. Experiments were performed at the NSLS, which is supported by the U.S. Department of Energy, Divisions of Materials and Chemical Sciences, under Contract No. DE-AC02-98CH10886. P.R. gratefully acknowledges financial support from the William V. Shannon Trust. T.D.M. acknowledges the support of DoD/ARPA under Grant No. MDA972-96-3-0014.

*Permanent address: School of Physical Sciences, Dublin City University, Dublin 9, Ireland.

†Author to whom correspondence should be addressed. Electronic address: ksmith@bu.edu

[1] S. Nakamura and G. Fasol, *The Blue Laser Diode: GaN Based Light Emitters and Lasers* (Springer, Berlin, 1997).

[2] F. A. Ponce and D. P. Bour, Nature (London) **386**, 351 (1997).

[3] *III-V Nitrides*, edited by F. A. Ponce, T. D. Moustakas, I. Akasaki, and B. A. Monemar, Mater. Res. Soc. Symp. Proc. No. **449** (Materials Research Society, Pittsburgh, 1997).

[4] H. Morkoc, S. Strite, G. B. Gao, M. E. Lin, B. Sverdlov, and M. Burns, J. Appl. Phys. **76**, 1363 (1994).

[5] H. Morkoc and S. N. Mohammad, Science **267**, 51 (1995).

[6] S. Strite and H. Morkoç, J. Vac. Sci. Technol. B **10**, 1237 (1992).

[7] *Photoemission in Solids*, edited by M. Cardona and L. Ley (Springer-Verlag, Berlin, 1978), Pts. 1 and 2.

[8] S. D. Kevan, *Angle Resolved Photoemission* (Elsevier, Amsterdam, 1991).

[9] K. E. Smith and S. D. Kevan, Prog. Solid State Chem. **21**, 49 (1991).

[10] V. M. Bermudez, D. D. Koleske, and A. E. Wickenden, Appl. Surf. Sci. **126**, 69 (1998).

[11] J. Nordgren and N. Wassdahl, Phys. Scr., T **T31**, 103 (1990).

[12] C. B. Stagarescu, L.-C. Duda, K. E. Smith, J. H. Guo, J. Nordgren, R. Singh, and T. D. Moustakas, Phys. Rev. B **54**, 17 335 (1996).

[13] K. E. Smith, L.-C. Duda, C. B. Stagarescu, J. Downes, D. Doppalapudi, R. Singh, T. D. Moustakas, J. Guo, and J. Nordgren, J. Vac. Sci. Technol. B **16**, 2250 (1998).

[14] L.-C. Duda, C. B. Stagarescu, J. Downes, K. E. Smith, D. Korakakis, T. D. Moustakas, J. Guo, and J. Nordgren, Phys. Rev. B **58**, 1928 (1998).
[15] D. Doppalapudi, S. N. Basu, K. F. Ludwig, Jr., and T. D. Moustakas, J. Appl. Phys. **84**, 1389 (1998).
[16] D. Doppalapudi, S. N. Basu, and T. D. Moustakas, J. Appl. Phys. **85**, 883 (1999).
[17] J. Nordgren and R. Nyholm, Nucl. Instrum. Methods Phys. Res. A **246**, 242 (1986).
[18] J. Nordgren, G. Bray, S. Cramm, R. Nyholm, J. E. Rubensson, and N. Wassdahl, Rev. Sci. Instrum. **60**, 1690 (1989).
[19] J. Nordgren, J. Phys. (France) **48**, 693 (1987).
[20] K. Lawniczak-Jablonska, T. Suski, I. Gorczyca, N. E. Christensen, K. E. Attenkofer, R. C. C. Perera, E. M. Gullikson, J. H. Underwood, D. L. Ederer, and Z. L. Weber, Phys. Rev. B **61**, 16 623 (2000).
[21] L. Bellaiche, T. Mattila, L. W. Wang, S. H. Wei, and A. Zunger, Appl. Phys. Lett. **74**, 1842 (1999).
[22] M. Katsikini, E. C. Paloura, J. Antonopoulos, P. Bressler, and T. D. Moustakas, J. Cryst. Growth **230**, 405 (2001).
[23] E. A. Albanesi, W. R. L. Lambrecht, and B. Segall, Phys. Rev. B **48**, 17 841 (1993).
[24] S. Pereira, M. R. Correia, T. Monteiro, E. Pereira, M. R. Soares, and E. Alves, J. Cryst. Growth **230**, 448 (2001).
[25] S. Pereira, M. R. Correia, T. Monteiro, E. Pereira, E. Alves, A. D. Sequeira, and N. Franco, Appl. Phys. Lett. **78**, 2137 (2001).
[26] M. D. McCluskey, C. G. Van de Walle, C. P. Master, L. T. Romano, and N. M. Johnson, Appl. Phys. Lett. **72**, 2725 (1998).
[27] C. G. Van de Walle, M. D. McCluskey, C. P. Master, L. T. Romano, and N. M. Johnson, Mater. Sci. Eng., B **59**, 274 (1999).
[28] I. Vurgaftman, J. R. Meyer, and L. R. Ram-Mohan, J. Appl. Phys. **89**, 5815 (2001).
[29] A. F. Wright and J. S. Nelson, Appl. Phys. Lett. **66**, 3051 (1995).
[30] M. Goano, E. Bellotti, E. Ghillino, C. Garetto, G. Ghione, and K. F. Brennan, J. Appl. Phys. **88**, 6476 (2000).
[31] W. R. L. Lambrecht, Solid-State Electron. **41**, 195 (1997).
[32] K. Osamura, S. Naka, and Y. Murakami, J. Appl. Phys. **46**, 3432 (1975).
[33] C. Wetzel, T. Takeuchi, S. Yamaguchi, H. Katoh, H. Amano, and I. Akasaki, Appl. Phys. Lett. **73**, 1994 (1998).
[34] J. Wagner, A. Ramakrishnan, D. Behr, M. Maier, N. Herres, M. Kunzer, H. Obloh, and K. H. Bachem, MRS Internet J. Nitride Semicond. Res. **4**, U111 (1999).
[35] K. P. O'Donnell, R. W. Martin, C. Trager-Cowan, M. E. White, K. Esona, C. Deatcher, P. G. Middleton, K. Jacobs, W. Van der Stricht, C. Merlet, B. Gil, A. Vantomme, and J. F. W. Mosselmans, Mater. Sci. Eng., B **82**, 194 (2001).
[36] E. V. Kalashnikov and V. I. Nikolaev, MRS Internet J. Nitride Semicond. Res. **2**, 18 (1997).
[37] R. Singh, D. Doppalapudi, T. D. Moutakas, and L. T. Romano, Appl. Phys. Lett. **70**, 1089 (1997).
[38] N. A. El-Masry, E. L. Piner, S. X. Liu, and S. M. Bedair, Appl. Phys. Lett. **72**, 40 (1998).
[39] T. Saito and Y. Arakawa, Phys. Rev. B **60**, 1701 (1999).
[40] J. Stöhr, *NEXAFS Spectroscopy* (Springer, Berlin, 1992).
[41] K. Lawniczak-Jablonska, T. Suski, Z. Liliental-Weber, E. M. Gullikson, J. H. Underwood, R. C. C. Perera, and T. J. Drummond, Appl. Phys. Lett. **70**, 2711 (1997).
[42] I. H. Ho and G. B. Stringfellow, in *III-V Nitrides* (Ref. 3), p. 871.
[43] I. H. Ho and G. B. Stringfellow, Appl. Phys. Lett. **69**, 2701 (1996).